X-ray photoelectron spectroscopy of Pd/γ-alumina and Pd foil after catalytic methane oxidation

L.P. Haack [1] and K. Otto

Ford Research Laboratory, Ford Motor Company, MD 3061/SRL, Dearborn, MI 48121-2053, USA

Received 30 December 1994; accepted 12 May 1995

Samples of palladium supported on γ-alumina and a palladium foil were used as catalysts for methane oxidation at 550°C. The samples were quenched quickly in the reaction chamber to room temperature in flowing Ar and then transferred in vacuo for XPS analysis. Structure sensitivity was manifest from an increase in PdO stability and a decrease in carbon deposition relative to Pd with increasing particle size. The results were compared with recent ellipsometric data.

Keywords: palladium; PdO; alumina; methane; oxidation; carbon; XPS; ellipsometry; structure sensitivity

1. Introduction

Recent progress in the stabilization of automotive catalysts by refined washcoat modifications makes it feasible to produce practical three-way catalysts (TWCs) that contain palladium as the only precious metal component. Palladium is also a preferred catalyst for the complete oxidation of methane [1], a hydrocarbon (HC) currently excluded from total HC emissions because of its low reactivity with atmospheric constituents. Since compressed natural gas (CNG) is an attractive alternate automotive fuel, except for its pronounced greenhouse effect, it is desirable to advance our basic knowledge of catalytic methane combustion. Earlier studies were based on X-ray photoelectron spectroscopy (XPS) [2], Raman spectroscopy [3] and ellipsometry [4]. The different methods serve to obtain comparable and complementary data to emphasize the value of in situ measurements. A recent investigation [4] showed the predominance of PdO on a palladium film during catalytic methane oxidation, even under reducing conditions. The study by XPS reported here provides additional data for the methane oxidation on palladium foil and extends the investigation to Pd particles supported on γ-alumina.

[1] To whom correspondence should be addressed.

2. Experimental

2.1. MATERIALS

Catalysts of Pd supported on γ-alumina were prepared at loadings of 0.5, 1.5 and 10 wt% by impregnation of γ-alumina with aqueous solutions of palladium nitrate. Pretreatment included calcination in air at 600°C for 20 h [3]. The samples were pressed into pellets for analysis by XPS. Pure Pd foil (99.99+%) was purchased from Goodfellow Metals.

2.2. XPS ANALYTICAL SYSTEM

XPS spectra were obtained using an M-Probe ESCA spectrometer manufactured by Surface Science Instruments, VG Fisons, with monochromatic Al Kα X-rays (1486.7 eV, 80 W) focused to a 1200 μm diameter beam. A low energy (1–3 eV) electron gun and a Ni charge neutralization screen placed 1–2 mm above the sample were employed to minimize surface charging effects [5]. The analyzer was operated at a 50 eV pass energy. To accurately determine Pd binding energies, a least-squares based fitting routine was used to peak-fit the Pd core level spectra when multiple states of Pd were present. This routine was allowed to iterate freely on the peak positions, integrated peak areas, and peak widths (FWHM). Pd 3d spectral curve fits represent the Pd $3d_{5/2}$ and Pd $3d_{3/2}$ spin–orbit splitting and therefore the Pd $3d_{5/2}$ and Pd $3d_{3/2}$ binding energy separation and intensity ratio were fixed to empirically determined values of 5.25 eV and 1.45, respectively. At low Pd concentrations, an average FWHM of 2.0 eV was achieved for the components of the peak fits. Only the binding energy value of the Pd $3d_{5/2}$ line is reported in this work. Binding energies were referenced to the Al 2p line at 74.2 eV, and measured to an accuracy of ±0.3 eV. C/Pd atomic ratios were determined using photoionization yields of the high resolution core level lines normalized by routines based on Scofield photoionization cross-section value [6]. A blank γ-alumina sample was analyzed along with the Pd/γ-alumina catalysts. The amount of carbon on this sample, measured after the same exposure time to the analysis chamber as the Pd/γ-alumina samples, was determined in order to subtract off the contribution of adventitious carbon (deposited during exposure to the analysis chamber) from carbon deposited during methane reaction.

The palladium materials were treated in a PHI model 04-800 reactor system mounted directly onto the introduction chamber of the spectrometer. A detailed description of this sample treatment system has been given previously [7]. Reactor gases were Ar (99.9995%), O_2 (99.98%) and CH_4 (99.8%), purchased from Matheson. Samples were pretreated for 2 h at 600°C in Ar containing 10% O_2 at a flow of 100 cm^3/min. The XPS Pd spectra obtained after oxidation pretreatment were the same as those shown in fig. 1, the initial oxidation reaction at $R = 0$, revealing that, as will be discussed later, the treatment converts all Pd in the sup-

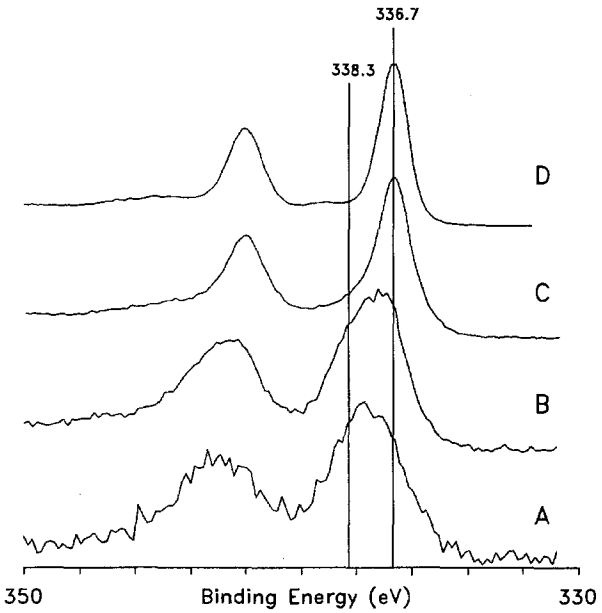

Fig. 1. XPS Pd 3d spectra of Pd catalysts cooled in argon after initial oxidation at 550°C; (A) 0.5 wt% Pd, (B) 1.5 wt% Pd, (C) 10.0 wt% Pd and (D) Pd foil. The spectra are the same when samples are cooled in oxygen and argon.

ported catalysts to oxide. The same treatment produces a PdO layer about 1000 Å thick on foils [8]. The samples were then exposed to selected mixtures of CH_4 and O_2 in Ar at 550°C for 4 h, cooled to 100°C in Ar and evacuated and transferred to the spectrometer analyzer chamber. Table 1 lists the reaction mixtures used. A redox potential R is defined by the ratio $[CH_4]/[2O_2]$. Thus, under ideal conditions, $R = 1$ is equivalent to a stoichiometric conversion of methane and oxygen to carbon dioxide and water. The samples were cooled in Ar to avoid extrinsic sample oxidation observed in mixtures of methane and oxygen once the

Table 1
Composition of gas mixtures

R-value	Gas flow (cm^3/min)			
	CH_4	O_2	Ar	total
0.0	0.0	30.0	270.0	300.0
0.10	2.5	50.0	247.5	300.0
0.25	5.0	40.0	255.0	300.0
0.50	5.0	20.0	275.0	300.0
0.80	5.0	12.5	282.5	300.0
1.0	5.0	10.0	285.0	300.0
1.5	5.0	6.7	288.3	300.0

methane oxidation stopped when the temperature dropped below the light-off point. Conversely, cooling of oxidized Pd from the reaction temperature to room temperature was fast enough to prevent decomposition of palladium oxide. It should be stressed that all the fully oxidized samples cooled in Ar alone yielded the same spectra, shown in fig. 1, obtained in a mixture of Ar and O_2. The samples were always transferred to the spectrometer in vacuo, at room temperature. This method eliminated contamination or oxidation by ambient air.

3. Results

Fig. 1 displays the XPS Pd 3d core level spectra of the three γ-alumina supported Pd catalysts and the Pd foil obtained after the initial oxidation reaction. The catalysts at low Pd loadings (0.5 and 1.5 wt%) showed Pd to be present in two distinct oxidation states. A previous XPS study of Pd supported on γ-alumina has revealed that the highest binding energy state of Pd (Pd $3d_{5/2}$ BE = 338.3) can be attributed to highly dispersed Pd in intimate contact with the alumina support [2]. This species is envisioned as either a support-stabilized PdO_2 (Pd^{4+}) or deficiently coordinated PdO (Pd^{2+}). The binding energy of the other Pd peak (Pd $3d_{5/2}$ BE = 336.7) is characteristic of particulate (bulk) PdO. The state of Pd at a loading of 10 wt% Pd and of the Pd foil after oxidation was exclusively PdO.

3.1. 0.5 wt% Pd ON γ-ALUMINA

The XPS Pd 3d core level spectra of the lowest loading catalyst after reactions with methane at redox potentials of $R = 0$ (pure O_2), 0.10, 0.25 and 0.50 are shown in fig. 2. At $R = 0$ (pure oxidizing atmosphere) Pd resided in a mixture of higher and lower binding energy oxidation states. At $R = 0.10$, Pd existed mostly in the 2+ state, with partial reduction to Pd^0. It is interesting that low temperature reduction in H_2 of dispersed palladium resulted in a similar binding energy downshift (or redistribution) in oxidized Pd species [2]. At the higher redox potentials of 0.25 and 0.50, Pd was reduced completely to the metallic state.

3.2. 1.5 wt% Pd ON γ-ALUMINA

XPS Pd 3d core level spectra at intermediate Pd loading after methane-oxidation catalysis are shown in fig. 3. At all redox potentials (higher than $R = 0$) Pd was reduced completely to the metallic state.

3.3. 10.0 wt% Pd ON γ-ALUMINA

In this case, Pd exists mostly in the particulate (bulk) phase. For reactions at $R = 0$ and $R = 0.10$, palladium remained completely as Pd^{2+} (fig. 4). At $R = 0.25$

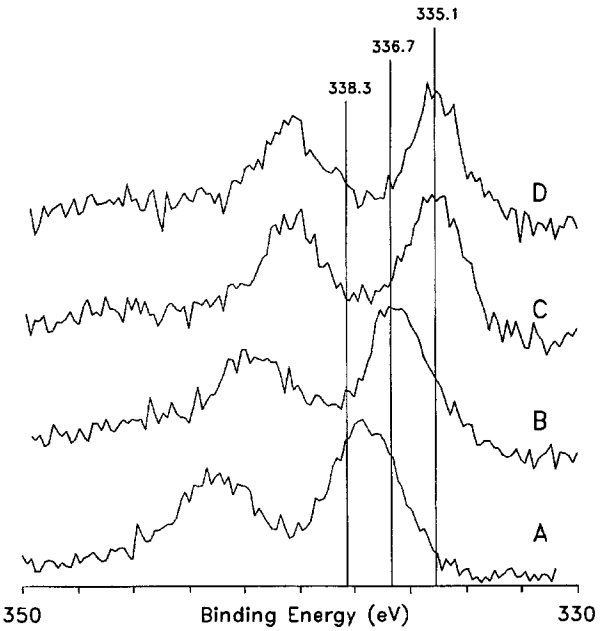

Fig. 2. XPS Pd 3d spectra of highly dispersed Pd (0.5 wt%) on γ-alumina after methane oxidation at (A) $R = 0$, (B) $R = 0.10$, (C) $R = 0.25$ and (D) $R = 0.50$.

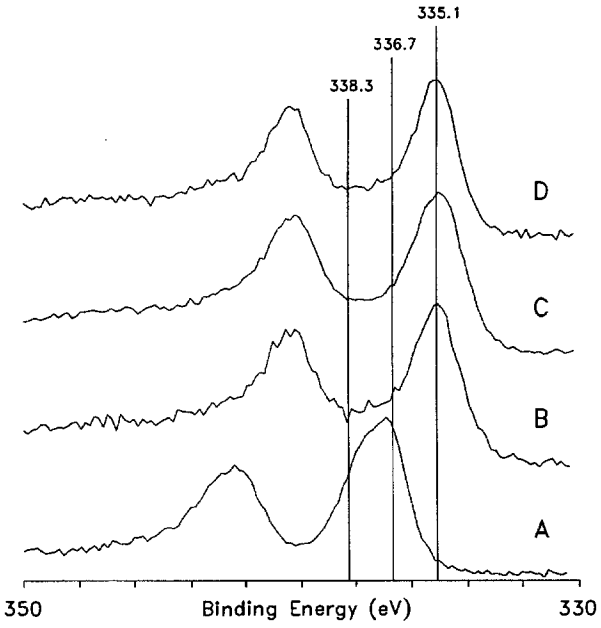

Fig. 3. XPS Pd 3d spectra of 1.5 wt% Pd on γ-alumina after methane oxidation at (A) $R = 0$, (B) $R = 0.10$, (C) $R = 0.25$ and (D) $R = 0.50$.

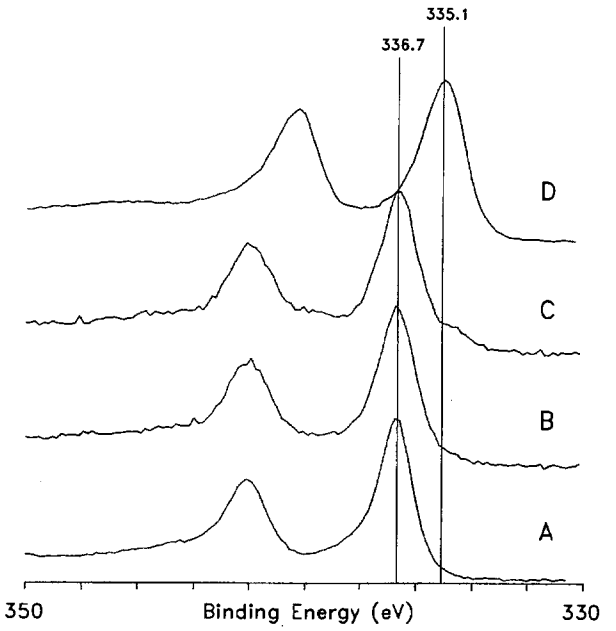

Fig. 4. XPS Pd 3d spectra of 10.0 wt% Pd on γ-alumina after methane oxidation at (A) $R = 0$, (B) $R = 0.10$, (C) $R = 0.25$ and (D) $R = 0.50$.

partial, but slight, reduction to metallic Pd occurred. Total reduction to metallic Pd was observed at $R = 0.50$.

3.4. Pd FOIL

At $R = 0$, 0.10 and 0.25 (fig. 5) and at $R = 0.50$ (not shown) XPS observed only PdO (Pd^{2+}). At stoichiometry ($R = 1.0$) a mixture of Pd^{2+} and Pd^0 was observed, accounting for a PdO : Pd ratio of 1.6.

Table 2 illustrates the change in PdO (Pd^{2+}) remaining after methane oxidation as a function of R-values greater than $R = 0$. The lowest loading of 0.5 wt% Pd is not included, since at the high dispersion Pd exists in two oxidation states Pd^{2+} and Pd^{4+} and thus complicates the analysis. For the same reason the value for 1.5 wt% at $R = 0.1$ is enclosed in parentheses to note the uncertainty of the analysis because of the presence of some residual Pd^{4+}.

4. Discussion

The results shown in table 2 demonstrate increasing predominance of PdO as the Pd concentration increases from 1.5 to 10 wt% and concomitantly the particle size increases. The highest degree of stability is observed for Pd foil. Predominance

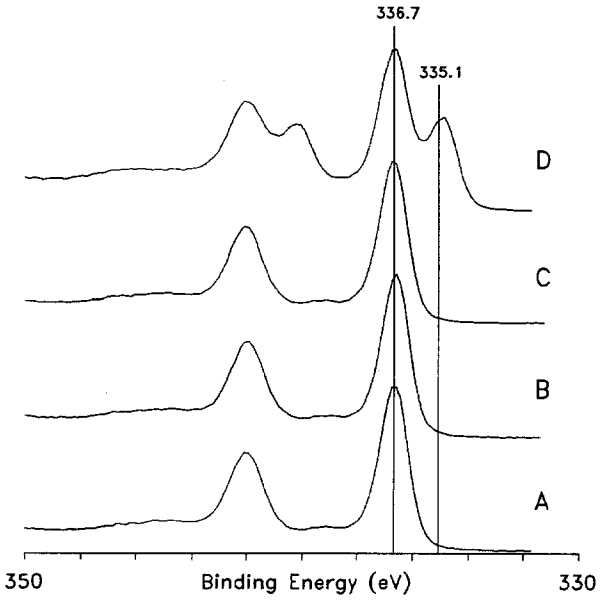

Fig. 5. XPS Pd 3d spectra of Pd foil after methane oxidation at (A) $R = 0$, (B) $R = 0.10$, (C) $R = 0.25$ and (D) $R = 1.0$.

of oxide on palladium foil, even under reducing conditions, was also observed in the ellipsometric study [4].

At the lowest concentration, 0.5, and to some extent at 1.5 wt% Pd, the catalyst shows different characteristics because of the postulated interaction with the alumina, as deduced earlier from XPS and Raman spectroscopy data [2,3]. The change in stability of PdO with particle size can be considered as a reason for the change of turnover rate that defines a structure sensitive reaction. Structure sensitivity of methane oxidation has been reported in the literature not only over Pd [9,10], but also over Pt [11], which does not form a bulk oxide. Ribeiro et al. [12] have stressed that in air, PdO, not Pd, is the stable bulk phase in the temperature range from 500 to 700°C. Hicks et al. [9,10] attributed the increase of turnover rate with particle size to a difference of oxygen bonding at the catalytic surface. They also found that the fraction of the bulk palladium oxidized increased with decreasing particle

Table 2
Percentage of palladium in the Pd^{2+} state

R-value	1.5 wt% Pd	10.0 wt% Pd	Pd foil
0.10	(9.3)	100	100
0.25	0	89.4	100
0.50	0	0	100
1.0	–[a]	–[a]	61.5

[a] Not measured.

size. Thus it can be assumed that the oxidation state of Pd plays a key role in the catalytic activity of Pd catalysts.

A second type of structure sensitivity as a function of Pd particle size is indicated for carbon deposition during methane oxidation. Plots of the C/Pd ratio derived from XPS spectra as a function of R-value are shown in fig. 6 for three palladium loadings of 0.5, 1.5 and 10 wt%. In fig. 6, the C/Pd ratio for Pd foil is marked by the triangles. The graph also serves to illustrate the data scatter. As expected, the carbon deposit intensifies in the R-value range from 0.5 to 1.5 wt%. However, adventitious carbon is a ubiquitous deposit, and, in fact, the C 1s line can be assigned as reference for the XPS analysis [13]. For an unambiguous analysis of carbon derived from the incomplete combustion of methane, it is necessary to subtract the contribution of the adventitious carbon. The results of this correction are summarized in table 3. The data scatter limits listed are standard deviations. In the R-range from 0 to 0.8, C/Pd = 0 within the experimental error and thus carbon deposits derived from methane are not measurable under these conditions. At higher R-values, carbon from incomplete methane oxidation is exceeding the error limits, especially at lower Pd loading. This carbon deposit decreases, relative to the amount of Pd, as the particle size increases with increasing Pd loading. On Pd foil, methane oxidation is essentially complete even at $R = 2$, and the C/Pd ratio shown in table 3 remains below 0.1.

Collectively it is seen that methane combustion becomes more efficient at higher palladium loadings when larger particles and a higher fraction of PdO exist. It is unclear to what extent loss of activity for highly dispersed palladium can be attributed to an interaction with the alumina, or to a higher metallic content [2]. But clearly, structure sensitivity is related to an increase in PdO stability with increasing particle size. It is interesting to note that Hicks et al. [10] speculated without experi-

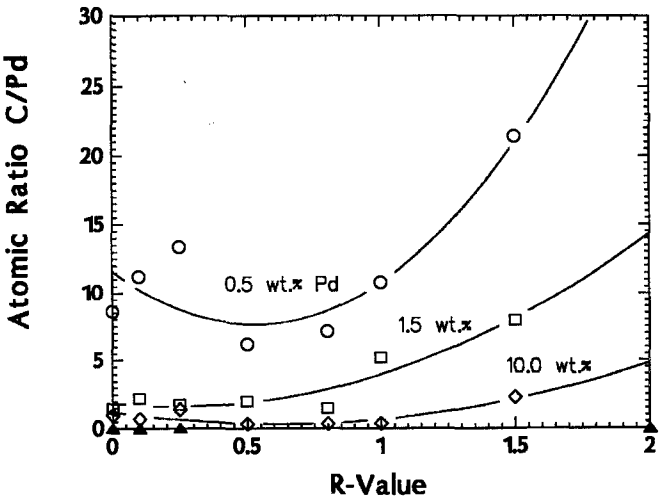

Fig. 6. The atomic C/Pd ratio as a function of redox potential and Pd loading.

Table 3
Atomic C/Pd ratio (multiplied by 100) attributable to incomplete methane oxidation as a function of Pd loading and R-value

wt% Pd	$R = 0$–0.8	$R = 1.0$	$R = 1.5$	$R = 2.0$
0	0	0	0	0
0.5	0.70 ± 3.0	2.2	13	–[a]
1.5	0.33 ± 0.3	3.8	6.5	–[a]
10.0	-0.22 ± 0.4	–0.60	1.3	–[a]
foil	0.01 ± 0.01	0.11	0.02	0.02

[a] Not measured.

mental evidence that poisoning of catalytic sites may explain deactivation of small Pd particles. The observed trend of carbon deposit as a function of particle size (see table 3) is consistent with such a conjecture.

A complete analysis of the surface chemistry of Pd during catalytic methane oxidation clearly requires detailed knowledge of oxygen transfer rates associated with the formation of H_2O, CO_2 and CO involving oxygen from the gas phase and the formation and dissociation of bulk PdO. It was observed that methane oxidation of Pd/γ-alumina continues when gas phase oxygen is depleted [14]. However, PdO as a methane oxidant oxidizes the carbon exclusively to CO, it produces no CO_2.

Comparison of XPS and ellipsometry data

In a recent study spectroscopic ellipsometry was used to follow the growth of a PdO layer on a Pd-film catalyst during methane oxidation [4]. The present investigation serves as another example to illustrate how XPS and ellipsometry can serve as complementary techniques to analyze catalyst surfaces under reaction conditions. The methods are not interchangeable since spectroscopic ellipsometry truly analyzes a catalyst under reaction conditions, while the XPS measurements are performed only quasi in situ. On the other hand, XPS is limited primarily to surface layers, while optical analyses probe a few hundred angstroms into the bulk. It should be noted that the two analytical methods also differ in as much as XPS measures atomic ratios while optical methods sample volume fractions. The most meaningful comparison between the two methods is for the Pd foil and the sputtered film employed in the ellipsometric analysis, considering the quantitative limitations mentioned.

Methane oxidation over Pd foil at the stoichiometric methane/oxygen ratio, $R = 1.0$, yields a layer of mostly PdO with a smaller amount of Pd metal. Ellipsometry showed evidence for only a few percent of reduced metal in this layer [4]. On the other hand, XPS indicated that 38% of the surface Pd was in the metallic state (PdO : Pd ratio of 1.6). Collectively these data indicate that the surface of the oxide layer has a significantly higher metallic content than the bulk.

Another complication, when comparing the two analytical methods, is an oscillation of the surface state during methane oxidation. Ellipsometry identified oscil-

lation between surface states rich in PdO and rich in Pd. Each state lasted a few minutes [4]. This is a commonly unrecognized pitfall. Unless an analysis is truly performed in situ, reproducibility has to be established by statistical means.

5. Conclusions

(1) XPS can be used to study the surface oxidation state of Pd supported on γ-alumina and of Pd foil after catalytic oxidation of methane. Since rapid cooling in Ar and transfer of the samples into the vacuum chamber prevented PdO decomposition, the analysis is considered quasi in situ.

(2) The stability of surface oxides increases with the size of Pd particles supported on γ-alumina and thus manifests a structure modification contributing to structure sensitivity of methane oxidation over Pd/γ-alumina.

(3) Structure sensitivity is also suggested by a change in carbon deposition derived from incomplete methane oxidation. Normalized to Pd, the intensity of the carbon deposit decreases with increasing Pd particle size. Carbon deposits are substantial for highly dispersed Pd on γ-alumina and for all supported samples at $R>1$.

(4) Ellipsometric analyses tend to indicate higher PdO concentrations than does XPS. The difference may be explained, in part, by the different sampling depths of XPS and optical probes.

Acknowledgement

We appreciate the review of this manuscript by our colleagues G.W. Graham, T.E. Hoost and W.H. Weber, and express our thanks for the revisions prompted by their comments.

References

[1] C.F. Cullis and B.M. Willa, J. Catal. 83 (1983) 267.
[2] K. Otto, L.P. Haack and J.E. deVries, Appl. Catal. B 1 (1992) 1.
[3] K. Otto, C.P. Hubbard, W.H. Weber and G.W. Graham, Appl. Catal. B 1 (1992) 317.
[4] D. König, W.H. Weber, B.D. Poindexter, J.R. McBride, G.W. Graham and K. Otto, Catal. Lett. 29 (1994) 329.
[5] C.E. Bryson III, Surf. Sci. 189/190 (1987) 50.
[6] J.H. Scofield, J. Electron Spectry. Relat. Phenom. 8 (1976) 129.
[7] L.P. Haack, J.E. deVries, K. Otto and M.S. Chattha, Appl. Catal. A 82 (1992) 199.
[8] J.T. Remillard, W.H. Weber, J.R. McBride and R.E. Soltis, J. Appl. Phys. 71 (1992) 4515.
[9] R.F. Hicks, H. Qi, M.L. Young and R.G. Lee, J. Catal. 122 (1990) 279.
[10] R.F. Hicks, H. Qi, M.L. Young and R.G. Lee, J. Catal. 122 (1990) 295.
[11] K. Otto, Langmuir 5 (1989) 1364.
[12] F.H. Ribeiro, M. Chow and R.A. Dalla Betta, J. Catal. 146 (1994) 537.
[13] L.P. Haack, C.R. Peters, J.E. deVries and K. Otto, Appl. Catal. A 87 (1992) 103.
[14] K. Otto and C.N. Montreuil, unpublished.